Available online at www.sciencedirect.com

ScienceDirect

Energy Procedia 148 (2018) 712–719

Energy Procedia

www.elsevier.com/locate/procedia

73rd Conference of the Italian Thermal Machines Engineering Association (ATI 2018), 12–14 September 2018, Pisa, Italy

Dynamic simulation of the temperature inlet turbine control system for an unfired micro gas turbine in a concentrating solar tower.

M. Amelio[a], M. Silva Pèrez[b], V. Ferraro[a], F. Rovense[a]*, S.Bova[a]

[a] *Department of Mechanical, Energy and Management Engineering, University of Calabria, Via P. Bucci Edificio Cubo 46 C, 87063, Arcavacata di Rende (CS), Italy*

[b]*Department of Energy Engineer, Escuela Técnica Superior de Ingeniería Universidad de Sevilla, Camino de los Descubrimientos, s/n. 41092 Sevilla, Spain*

Abstract

In this work, the dynamic performance of a mass flow regulation system, in a concentrating solar tower plant, with unfired closed micro gas turbine, during clouds transient will be presented. The adjustment system operates with the heliostats field control system, in order to control the temperature inlet turbine. To choose the best configuration, the performance of three heliostats sizes, for four Solar Multiple, has been evaluated. The design of the solar field was carried out by means of Solar Pilot, while the numerical models have been developed in Matlab/Simulink. The results show that a particular configuration is suitable for this purpose.

Keywords: Concentrating Solar Tower, Micro Gas Turbine, TIT, Mass Flow Regulation System, Heliostats Field

* Corresponding author.
E-mail address: francesco.rovense@unical.it

10.1016/j.egypro.2018.08.161

1. Main text

Nowadays, the use of renewable sources plays a fundamental role in the energetic systems research as well as their effects on the National Grid performance once integrated [1]. The solar source is the most exploitable one and can be used to generate energy in different ways or to produce fuels as a storage option [2]. One of these ways is the concentrating solar technology, which is able to increase the temperature of a heat transfer fluid in a thermodynamic cycle in order to produce electric energy. In the last years, many projects and researches have demonstrated the effectiveness of the solar gas turbine systems [3,4] together with the integration of district and regional energy systems to enhance the sustainability levels of industry and buildings' consumption [5]. Solar energy systems can indeed play the role of a viable alternative to the well-established gas-based systems for energy supply [6]. In past works the use of air as heat transfer fluid (HTF) in solarized gas turbine was explored [7,8]. In this work, the dynamic performance of the regulations systems, during thermal load transient due to the clouds transfer, sunrise and sunset will be presented.

Nomenclature

SM	Solar Multiple
TIT	Temperature Inlet Turbine [°C]
DNI	Direct Normal Irradiance [W/m^2]
HTF	Heat Transfer Fluid
CSP	Concentrating Solar Power
μGT	Micro Gas Turbine
$\dot{m}_{min}$	Minimum mass flow rate under ambient pressure [kg/s]
$\dot{m}_{\max}$	Maximum value of mass flow rate under pressurized condition [kg/s]
Q_{th}	Required thermal power [kW]
Φ_{avg}	Average flux incident [kW/m^2]
ρ_{air}	Air density [kg/m^3]
Q_{inc}	Incident thermal radiation [kW]
Q_{loss}	Thermal loss [kW]
Q_{wf}	Thermal power transfer to the HTF [kW]
m	Absorber air mass [kg]
c_p	Specific heat [kJ/kg °C]
ρ	Density of the material [kg/m^3]
p	Porosity of the material
η_{SF}	Efficiency of the heliostat field [-]
A_{SF}	Effective area of the heliostats field [m^2]
A_{eff}	Heliostat effective area focused on the receiver [m^2]
$\phi(t)$	Instantaneous incident flux f(DNI, η, SF) [kW/m^2]
ΔT	Instantaneous temperature variation [°C]
ΔT_{lim}	Limit difference of temperature [°C]
Q_{inc}	Incident power related to heliostats area A'_{eff} [kW]
A'_{eff}	Discretized heliostats area [m^2]
T_{amb}	Ambient temperature [°C]
ε	Emission coefficient (0.96)
α	Absorption coefficient
s	Thickness of the thermal insulator, 0.1 m (stone wool)
K	Thermal conductibility of the insulator (stone wool) (0.1134 W/mK)
$\dot{m}_{air}$	Air mass flow crossing the receiver [kg/s]
h_{out}	Air enthalpy outlet from the receiver [kJ/kg]
h_{in}	Air enthalpy inlet in the receiver [kJ/kg]
ϕ_{min}	Minimum flux incident (144.5 kW/m^2)
$\dot{m}(t)$	Instantaneous mass flow rate [kg/s]

η_{el}	Electric efficiency (0.97) [-]
η_{mec}	Mechanical efficiency (0.94) [-]
$h_{in,t}$	Air enthalpy inlet turbine [kJ/kg]
$h_{out,t}$	Air enthalpy outlet turbine [kJ/kg]
$h_{in,c}$	Air enthalpy inlet compressor [kJ/kg]
$h_{out,c}$	Air enthalpy outlet compressor [kJ/kg]

1.1. Plant description

In previous works, the authors analyzed the use of the temperature inlet turbine (TIT) control system, performed by the mass flow adjustment, for an unfired micro gas turbine in a solar tower plant [17]. The plant, as shown in figure, 1 is composed by a regenerated micro gas turbine (μGT), a solar tower, receiver, heliostats field, mass flow regulation system (bleed valve, auxiliary compressor) and cooling system. The control system performs, varying the mass flow rate by a base pressure variation; this variation is acted by the auxiliary compressor and a bleed valve, depending on the Direct Normal Irradiance (DNI) in order to control the TIT around the value of 800°C [9].

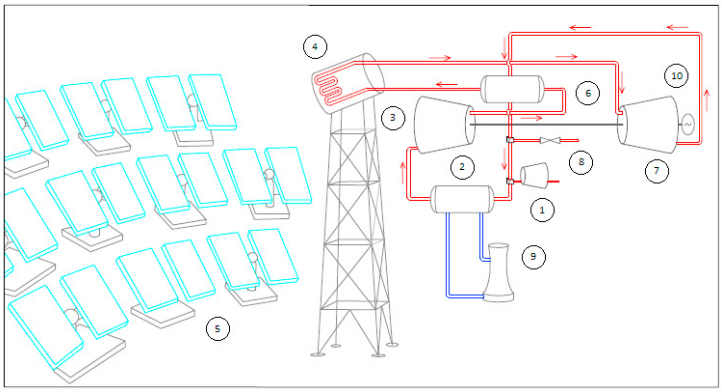

Fig. 1. Power plant scheme: 1. Auxiliary compressor; 2. Low temperature heat exchanger; 3. Compressor; 4. Receiver; 5. Heliostats field; 6. Regenerator; 7. Turbine; 8. Bleed valve; 9. Cooling tower; 10. Electric generator.

The mass flow regulation system operates together with the heliostats field control system, in order to adjust the flux, around the average value of 400 kW/m^2 [10] on the receiver, influencing also the TIT. In table 1 there are the main data of the solar power plant.

Table 1. Main data of power plant

Location	Seville
Nominal power [kW]	500
Pressure ratio μGT	4.5
Pressure ratio auxiliary compressor	5
Minimum inlet compressor pressure [bar]	1.013
Minimum outlet compressor pressure [bar]	4.559
Minimum turbine inlet pressure [bar]	4.314
Maximum inlet compressor pressure [bar]	5.065
Maximum outlet compressor pressure [bar]	22.795
Maximum turbine inlet pressure [bar]	21.570
Minimum mass flow rate [kg/s]	0.9165
Maximum flow rate [kg/s]	4.5564

2. Methodology

In this part, numerical modelling of the entire power plant will be depicted. Simulink® / MATLAB® was the tool used to simulate and analyze the dynamic behavior. Therefore, the control system has been modelled by varying the mass flow rate in order to compensate the DNI variations and to maintain almost constant the TIT.

Since gas turbines operate in optimal conditions only for a particular ratio between the rotation speed and the working fluid speed, this ratio must be kept constant. The rotation speed does not change as well as the velocity triangles and the volumetric flow rate. With a variable density working fluid, the system can therefore operates at variable mass flow rate, maintaining the optimal operating conditions. The mass flow variations in the cycle, for the adjustment of the TIT due to the variation of the thermal load (intercept by the CSP system), are caused by the air density variation. This effect is obtained through the air pressure variation at the inlet section of the μGT compressor. The relation between these two variables could be expressed by the Ideal Gas Law.

In table 2 the main data of the tree heliostats type analyzed in this work [11] are reported, while in table 3 there are the thermal power and number of heliostats for each SM. The efficiency matrix and solar field design were performed employing SolarPilot, and the results were used in the numerical model to evaluate the solar field performance [12].

Table 2. Heliostats dimension data

	Type 1	Type 2	Type 3
Area [m^2]	115.56	43.33	16.69
Height [m]	9	6.42	3.21
Length [m]	12.84	6.75	5.2
Number of panel X direction [-]	4	3	2
Number of panel Y direction [-]	4	2	1

Table 3. Heliostats filed main data

SM	Q_{field}	#Heliostats type 1	#Heliostats type 2	#Heliostats type 3
1	1.7	31	76	206
1.1	1.87	33	82	223
1.2	2.04	36	88	241
1.3	2.2	39	94	257

2.1. Receiver

As the system works under pressurized conditions, an employing of volumetric pressurized receiver have been supposed. Another important device is the quartz window on the receiver aperture. The main reason of this choice is the requirement of reducing thermal radiative losses. The volumetric effect of this kind of receivers allows obtaining losses reductions, despite the high temperature inside the material. The absorber is made of Silicon Carbide (SiC), ceramic material with excellent radiative and thermal properties, able to withstand temperatures of 1400 ° C [13].

The aperture of the receiver, which depends on the solar energy intercepting, and the thermal losses values are expressed as:

$$A_{ar} = \frac{Q_{th}}{\Phi_{avg}} \qquad (1)$$

2.2. Heat balance equation

The equation on which is based the model, is the balance of the absorber inlet and outlet thermal power:

$$\frac{dU}{dt} = Q_{inc} - Q_{loss} - Q_{wf} \qquad (2)$$

Introducing the thermal capacity, the internal energy variation (3) will be expressed as function of the temperature variation:

$$\frac{dU}{dt} = m\, c_p \frac{dT}{dt} \qquad (3)$$

It was assumed to employ a flat plate-shaped absorber, with a porous honeycomb structure. This is characterized by a frontal area equal to the aperture of the receiver and a thickness of 9.5 cm.

Assuming a porosity of 49.51% [14], and considering that the density of silicon carbide is 3.21 g/cm3, the mass of the absorber is:

$$m = \rho V(1-p) \qquad (4)$$

The heat capacity (C) has been evaluated as the product between c_p (1.2 kJ/kg °C) [15] and the mass (m):

$$C = c_p \rho V(1-p) \qquad (5)$$

While the superficial average temperature of the absorber is:

$$\bar{T}_{abs} = \int \frac{1}{C}\frac{dU}{dt} \qquad (6)$$

This temperature has been assumed equal to that of the air leaving the receiver.

2.3. Incident power

The power incident is mainly function of direct normal radiation (DNI), heliostats field efficiency and reflective heliostats total area. DNI and field efficiency depends on the azimuth and zenith, which, in this model, are the input data with a one-minute step. The incident power in the model was evaluated as follows:

$$Q_{inc,t} = \eta_{SF}\, DNI\, A_{SF} \qquad (7)$$

2.4. Heliostat field

Using the power of the heliostats field, the code calculates the average flux that theoretically affects the absorber. In the case where this value is higher than the average flux set , the air coming out from the receiver exceeds the fixed value of 800 ° C. At this point, the maximum mass flow is flowing and therefore, it is not possible to remove excess heat from the receiver. To keep the constant air temperature, a part of the heliostats is then defocused; this is an operation that maintains the average incident flux on the receiver at the set values. The percentage of heliostats focused i.e. the focusing factor F_ϕ, have been evaluated as:

$$F_\phi = \frac{A_{eff}}{A_{SF}} = \frac{\phi_{avg}}{\phi\,(t)} \qquad (8)$$

From equation 8 it can be noticed that the relation between the area of the heliostats that must be focused on the receiver and the nominal area of the field is also expressed as a ratio between the fluxes. The absorber incident flux is equal to the ratio between the instantaneous incident power and the aperture receiver area A_{ar}:

$$\phi(t) = \frac{\eta_{SF}\, DNI\, A}{\mathrm{A_{ar}}} \qquad (9)$$

Therefore, the flux $\phi(t)$ is associated to the nominal area, while the average flux ϕ_{avg}, is associate to the

instantaneous surface, necessary to prevent to exceed this limit value. By the ratio between the fluxes, it is obtained the effective area of the heliostats field.

There is also a second defocusing type, based on the temperature derivative, which is carried out to prevent the overshoot of the TIT, due to rapid increases of solar radiation, in flux conditions lower than the design average value. This second focusing factor (FT) is expressed as:

$$F_T = 2 - \frac{\Delta T}{\Delta T_{lim}} \qquad (10)$$

Additionally, as the heliostats are defocused due to the rapid increase in temperature, in the next step not all are focused on the receiver, but only a percentage. The reason why is to avoid temperature fluctuations that could arise a sudden refocus of a large amount of heliostats. Only 5 % of the heliostats defocused then will be active.

In each calculation loop, the code compares the two focusing factors, by choosing the lower value, in order to evaluate the heliostats area. The area value, evaluated from this comparison, requires a discretization, because is not a discrete number but only a percentage of defocusing area.

$$Q_{inc} = Q_{inc,t} \frac{A'_{eff}}{A_{SF}} \qquad (11)$$

2.5. Thermal losses

There are radiative and conductive losses in the receiver, but convective losses, due to the quartz window, installed in the receiver aperture, are neglected [11]. The thermal losses could be expressed as:

$$Q_{loss} = Q_{rad} + Q_{cond} = \varepsilon\sigma A_{ar}(\bar{T}_{abs}^4 - T_{amb}^4) + K \frac{A}{s}(\bar{T}_{abs} - T_{amb}) \qquad (12)$$

In the case of conductive losses, it is assumed that these occur through the case of the receiver cavity. It was supposed that the receiver had a performance of a grey body (ε=α).

2.6. Power to heat transfer fluid

The power absorbed by the air, during the passage of the porous matrix, is the function of the mass flow rate that flows in the cycle and of the enthalpy difference of the air incoming and out coming from the receiver:

$$\mathrm{Q_{wf}} = \dot{\mathrm{m}}_{\mathrm{air}} (\mathrm{h_{out}} - \mathrm{h_{in}}) \qquad (13)$$

2.7. Mass flow air

The air flow rate flowing in the cycle, has been modelled in order to vary both as a function of the incident flux on the receiver, to maintain a constant TIT, both in function of the temperature of the receiver, to simulate the transient start-up and shutdown of the plant.

The flow rate in the two conditions were evaluated as the product of the volumetric flow rate V, constant during all the different operating conditions, and the density of air.

$$\dot{m}_{air} = \rho_{air}(p,t)V \qquad (14)$$

Once the minimum flow rate has been reached, the flux adjustment is carried out. This allows to keep constant the TIT value, regulating the thermal power absorbed by the fluid, by a mass flow rate variation. As the control strategy, has been established that, the mass flow rate varies linearly with the incident flux on the absorber, according to the following equation:

$$\frac{\dot{\mathrm{m}}(\mathrm{t}) - \dot{\mathrm{m}}_{\mathrm{min}}}{\dot{\mathrm{m}}_{\mathrm{max}} - \dot{\mathrm{m}}_{\mathrm{min}}} = \frac{\phi(\mathrm{t}) - \phi_{\mathrm{min}}}{\phi_{\mathrm{avg}} - \phi_{\mathrm{min}}} \qquad (15)$$

2.8. Power production

The net electric power P_{net} generated by the power unit is calculated as the difference between the power produced by the turbine and the power absorbed by the compressor. Both powers are functions of the air enthalpy at inlet and outlet of the components:

$$P_{net} = \eta_{el}\, \dot{m}_{air} \left[\eta_{mec}\left(h_{in,t} - h_{out,t}\right) - \frac{1}{\eta_{mec}}\left(h_{in,c} - h_{out,c}\right)\right] \quad (16)$$

The enthalpy values of the equation 15 from Matlab library have been used.

3. Results

In this section will be shown the model results to illustrate as the two controls system perform together, in order to control the TIT and the power produced. The data are referred to the 21st of June of TMY3 data of Seville [16].

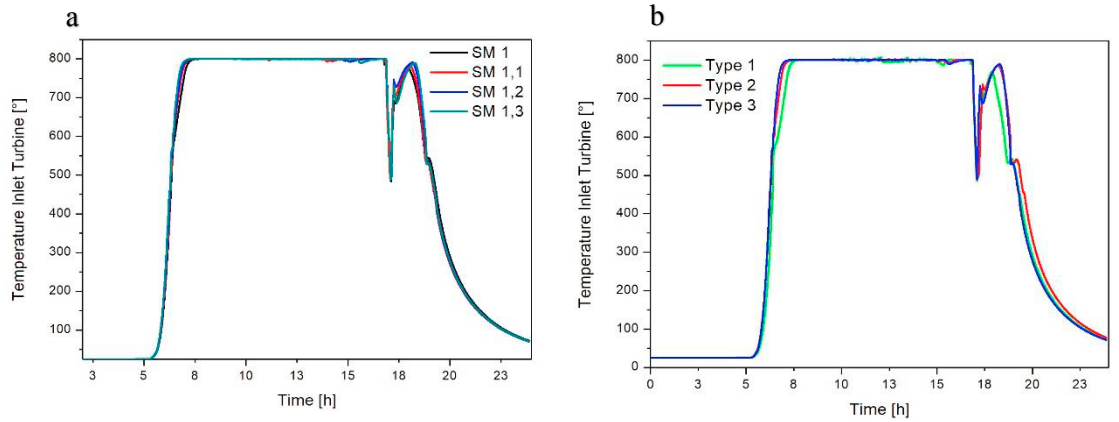

Fig. 2. (a) TIT trend for heliostats type 3; (b) TIT trend for SM 1 configuration.

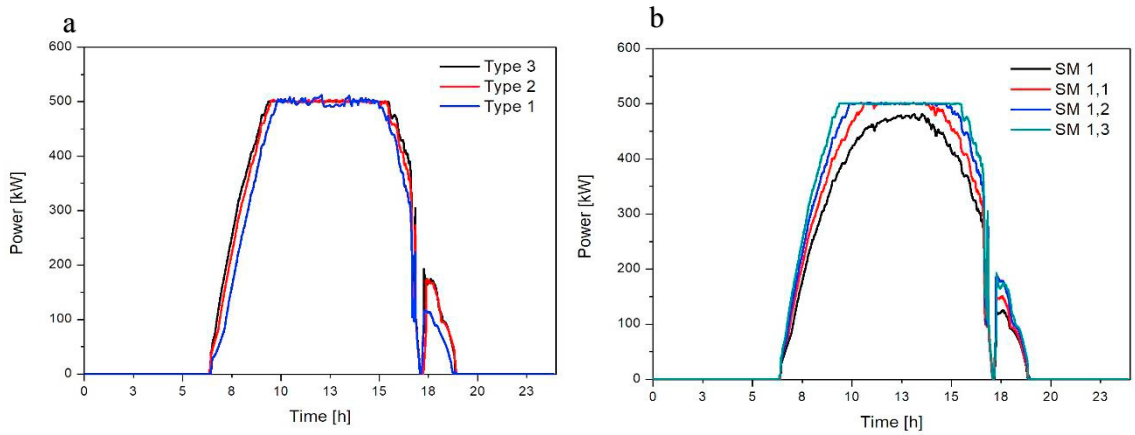

Fig. 3. (a) Power production trend for heliostats type 3; (b) Power production trend for SM 1.3 configuration.

As it is possible to notice from figure 2a, the mass flow regulation system performs during sunrise, sunset or during clouds transient (around17:00 PM in the considered day), while from 6 AM to 16.30 PM the TIT control is acted by the defocusing heliostats field control system. Particularly SM 1.3 configuration, allows to keep constant for more time the TIT. In addition, as shown in figure 2b, smaller heliostats (type 3) are the more able to control the TIT; they manage to warm up more quickly the receiver and loosen the cooling.

As it can be possible to observe in figure 3a, the SM 1.3 configuration allows to increase the energy production and simultaneously control the power, while, as shown in figure 3b, the best power control is acted by heliostats type 3 (smaller).

4. Conclusions

In this work, a dynamic model of the solar power plant with an unfired closed micro gas turbine, employing the mass flow regulation system has been analyzed. A numerical model in Matlab/Simulink has been developed in order to estimate the behavior of the plant under transient conditions. In the model, the heliostats regulation system have been implemented, in order to control the average incident flux on the receiver, which performs with the mass flow control system. The results show as the best configuration has SM 1.3 with smaller size heliostats (type 3); this configuration allows producing 1.08 MWh/year, with an efficiency almost constant to 30% and a utilization factor of 25% without use of fuel or employing of thermal storage.

Acknowledgements

Special thanks to Matteo Gallina for his precious support and to researchers of the Thermodynamics Department of University of Seville for their essentials suggests

References

[1] Noussan, M.; Roberto, R.; Nastasi, B., *Performance Indicators of Electricity Generation at Country Level—The Case of Italy*. Energies 2018, 11, 650.

[2] Astiaso Garcia, D.; Barbanera, F.; Cumo, F.; Di Matteo, U.; Nastasi, B. *Expert Opinion Analysis on Renewable Hydrogen Storage Systems Potential in Europe. Energies 2016, 9, 963.* https://doi.org/10.3390/en9110963

[3] M. Quero, R. Korzynietz. M. Ebert, AA. Jiménez, A. del Río, JA. Brioso. Solugas – *Operation experience of the first solar hybrid gas turbine system at MW scale*. SolarPACES 2013 Energy Procedia Volume 49, 2014, Pages 1820-183.

[4] P. Heller, M. Pfänder, T. Denk et al., 2006, *Test and Evaluation of a Solar Powered Gas Turbine System, Solar Energy, Volume 80, pp. 1225 – 1230.*

[5] Livio de Santoli, Francesco Mancini, Benedetto Nastasi, Serena Ridolfi, *Energy retrofitting of dwellings from the 40's in Borgata Trullo - Rome*, Energy Procedia, Volume 133, 2017, Pages 281-289, ISSN 1876-6102, https://doi.org/10.1016/j.egypro.2017.09.389

[6] Noussan, M.; Nastasi, B. D*ata Analysis of Heating Systems for Buildings—A Tool for Energy Planning, Policies and Systems Simulation*. Energies 2018, 11, 233. https://doi.org/10.3390/en11010233

[7] Rovense F., *A case of study of a concentrating solar power plant with unfired Joule-Brayton cycle*. Energy Procedia Vol 82 Pag. 978 – 985 (2015).

[8] Rovense F., Amelio M., Ferraro V., Scornaienchi N.M. (2016). *Analysis of a concentrating solar power tower operating with a closed joule Brayton cycle and thermal storage*, International Journal of Heat and Technology, Vol. 34, No. 3, pp. 485-490. DOI: 10.18280/ijht.340319

[9] William B. Stine and Michael Geyer (2001). *Power from the sun*. http://www.powerfromthesun.net/book.html.

[10] A. L. Ávila-Marín, *Volumetric receivers in solar thermal power plants with central receiver system technology*, Solar Energy, 2011; Volume 85, Issue 5: Pag. 891-910

[11] F. Téllez, M. Burisch, Villasente, M. Sánchez, C. Sansom, P. Kirby, P. Turner, C. Caliot, A. Ferriere, C A. Bonanos, C. Papanicolas, A Montenon, R.Monterreal, J.Fernández, *State of the Art in Heliostats and Definition of Specifications*, STAGE STE Projec, Deliverable 12, 2014.

[12] F. Rovense, M. Bomentre, M.S.Silva, V. Ferraro1, M.Amelio, *Design of heliostat field for an unfired solarized micro gas turbine in a closed cycle with mass flow control regulation, Under Press*

[13] F. Gomez-Garcia, J.González-Aguilar, G. Olalde, M. Romero, *Thermal and hydrodynamic behavior of ceramic volumetric absorbers for central receiver solar power plants: A review, 2016.*

[14] R. Pitz-Paal, B. Hoffschmidt, M. Bohmer, M. Becker, *Experimental and numerical evaluation of the performance and flow stability of different types of open volumetric absorbers under non-homogeneous irradiation, Solar* Energy 60, 135-150, 1997.

[15] W.Janke, A. Hapka, *Nonlinear thermal characteristics of silicon carbide devices*, Materials Science and Engineering B 176, pag. 289–292, 2011.

[16] Moreno T.S., et al. *Solar resource assessment in Seville, Spain, statistical characterisation of solar radiation at different time resolutions*, Solar Energy, Vol. 132, pp. 430-441. (2016)

[17] F.Rovense, M.Amelio, N.M. Scornaienchi, V.Ferraro, *Performance analysis of a solar-only gas micro turbine, with mass flow control* Energy Procedia Vol. 126 Pag. 675–682.